Strengthening adhesion of polycarbazole films on ITO surface by covalent electrografting of monomer

Abhishek Kumar, Emmanuel Contal, Sophie Lakard, Frédéric Dumur, Rita Meunier-Prest, Lydie Viau, Marcel Bouvet, Boris Lakard

Strengthening adhesion of polycarbazole films on ITO surface by covalent electrografting of monomer

Abhishek Kumar[1], Emmanuel Contal[2], Sophie Lakard[2], Frédéric Dumur[3], Rita Meunier-Prest[1], Lydie Viau[2], Marcel Bouvet[1], Boris Lakard[2]*

[1] Univ. Bourgogne Franche-Comté, ICMUB, UMR CNRS 6302, 21078, Dijon, France

[2] Univ. Bourgogne Franche-Comté, Institut UTINAM, UMR CNRS 6213, 25030, Besançon, France

[3] Aix Marseille Univ, CNRS, ICR, UMR 7273, F-13397 Marseille, France

---

Email addresses and ORCID number of authors (corresponding author email is marked with asterisk)

abhishek.Kumar@u-bourgogne.fr (ORCID no. 0000-0002-4306-9644)

emmanuel.contal@univ-fcomte.fr (ORCID no. 0000-0003-0146-589X)

sophie.lakard@univ-fcomte.fr (ORCID no. 0000-0001-9846-6893)

frederic.dumur@univ-amu.fr (ORCID no. 0000-0003-4872-094X)

rita.Meunier-Prest@u-bourgogne.fr (ORCID no. 0000-0001-5597-3879)

lydie.viau@univ-fcomte.fr (ORCID no. 0000-0002-2403-5692)

marcel.bouvet@u-bourgogne.fr (ORCID no. 0000-0002-2272-6633)

* boris.lakard@univ-fcomte.fr (ORCID no. 0000-0001-9686-4978)

Abstract: Strong adhesion of a functional polymer coating to a solid support is a key requirement to achieve its robustness and high performance in different application areas. Herein, a novel carbazole derivative, 9-methyl-9*H*-carbazole-3,6-diamine (m-Cz-diamine), is synthesized and covalently grafted onto an ITO surface through the diazonium electroreduction method. The functionalization of the ITO surface is confirmed by XPS spectroscopy, water contact angle measurements and cyclic voltammetry analysis, revealing the covalent anchoring of an organic film (m-Cz-ITO). The functionalized ITO surface is then studied for oxidative electropolymerization of m-Cz-diamine and carbazole, showing clear advantages over a bare ITO substrate in terms of polymer film adhesion. The polymer films electrodeposited onto an electrografted ITO surface demonstrate very strong adhesion, as they do not delaminate, either by a scotch tape pulling, storing in air, or immersing under water for two months. On the other hand, the polymer films grown on a bare ITO substrate peel off easily in all the aforementioned stability tests. Therefore, electrografting an organic film onto the ITO surface clearly improves the adhesion of the polymer films on top of it. Moreover, it is interesting to note that the physicochemical properties of the polymer films deposited on the functionalized ITO substrate remain unchanged.

Keywords: Carbazoles; Conducting polymers; Diazonium; Electrochemistry; Electrografting; Thin films.

---

1. Introduction

The research area of π-conjugated polymers has drawn numerous research interests since the pioneering work of Lethebyin to obtain polyaniline (PANI) by electrochemical oxidation of aniline in acidic media [1]. In the following years, multitudes of conducting polymers were electrosynthesized as exemplified with polyacetylene [2], polypyrrole [3] and polythiophene [4] among others. These polymers have been used in diverse applications, owing to their outstanding magnetic [5], electrical [6] and optical [6] properties. They possess a low-energy optical transition, tunable electrical conductivity, high electronic affinity and good mechanical flexibility, which make them the material of choice for applications in electrochemical sensors [7, 8], biosensors [9, 10], supercapacitors [11], fuel cells [12], batteries [13] and optoelectronic devices, such as solar cells [14]. However, a commonly encountered problem, while coating a surface through *in situ* electropolymerization is the weak adhesion between the organic layer and the substrate. This is because polymer chains formed near the electrode-electrolyte interface are immobilized on the electrode surface through physisorption, which is rather a weak interaction. Such weak and unstable adhesion of conducting polymers to substrates often results in interfacial failures and consequent loss of functionality, which adversely affects the reliability and efficiency of devices [15, 16]. With thicker conjugated polymer films the problem of poor adhesion is amplified [17]. A few previous literature studies also reported that conducting films may even completely delaminate from the substrate to form free-standing membranes [18, 19]. To overcome this challenge, several surface functionalization methods have been explored, in which a common strategy has been to strengthen the adhesion of the polymer layer through formation of a stronger covalent bond.

One approach to overcome the poor adhesion is to use bifunctional molecules to form self-assembled monolayers (SAMs) on the metal substrate (gold, platinum) through the well-known thiol chemistry. Thus, a SAM of monomer-functionalized thiols coated onto gold or platinum

substrates resulted in improved adhesion of subsequently deposited conducting polymers [20, 21]. Covalent bonding on substrates can also be achieved using monomer-functionalized silanes to form chemical bonds with metals or metal oxides. This strategy was first used by Simon *et al*., reporting covalent anchoring of *N*-(3-trimethoxysilyl-propyl)pyrrole on platinum or silicon electrodes *via* reaction with surface -OH groups. On the functionalized electrodes, the pendant pyrrole groups of the organosilane acted as initiation sites for the polymerization of polypyrrole [22]. Such a surface modification allowed to improve the adhesion and mechanical stability of polypyrrole films without degrading their conductivity and electroactivity [23], which promoted their applications in anticorrosion coatings [24, 25]. Similarly, adsorption of polyaniline on titania or silica particles can be achieved by pre-grafting an organosilane through the -OH groups of the particles, followed by polymerization to generate the polymer shell. In this manner, 3-aminopropyl(triethoxysilane) and *N*-[(3-trimethoxysilyl)-propyl]aniline have been used for the preparation of SiO_2@PANI [26, 27] and TiO_2@PANI particles [28, 29].

Chemical [30, 31] or electrochemical [32, 33] reduction of diazonium derivatives is another versatile technique for surface functionalization of substrates, imparting robust film adhesion through the formation of carbon-metal [34] or carbon-oxygen covalent bonds [35]. In this approach, an aryldiazonium salt precursor is at first electrochemically/chemically reduced into reactive free-radical, that is subsequently covalently grafted on the surface of the substrate [36, 37]. This strategy has several advantages compared to the SAM and silanization methods. For instance, the associated chemical/electrochemical reactions in grafting through diazonium reaction are easier to control and thus film thickness can be effectively controlled. Additionally, there are ample possibilities, based on amide coupling, click chemistry, coordination bonding among others to further modify the surface functionality suited for post-functionalization grafting of polymer chains [38]. In particular, the high stability of the modified surfaces induced

by the electroreduction of diazonium salts exhibited a decisive advantage for the stability of biosensors [39-43] and energy storage devices [44-46].

Conducting polymer films have already been obtained from various aryldiazonium derivatives. Polyaniline films were prepared by Vacca *et al.* onto gold substrates through a three steps process [47]. At first, a gold electrode was functionalized with 4-nitrophenyl by electrochemical reduction of 4-nitrobenzenediazonium salts. Subsequently, nitro groups were electrochemically reduced to amine groups, which were finally used as an initiator for the electropolymerization into polyaniline film. The modification of electrodes with aminophenyl groups can also be achieved by one-step procedure, involving the direct electroreduction of 4-phenylaminodiazonium in acidic medium [48]. Using this direct approach, Santos *et al.* reported the electropolymerization of diphenylamine into covalently-linked polyaniline film on glassy carbon electrode, in which the resulting film demonstrated improved chemical stability under high temperatures and ultrasonication [49]. Pilan *et al.* also used an electrografted layer of aminophenyl moieties to prepare polyaniline / carbon nanotube composites, exhibiting a significantly improved stability and higher capacitance values [50]. The electropolymerization of pyrrole was achieved on Ni and NiTi alloy substrates, which were pre-grafted with 4-pyrrolylbenzene via electroreduction of 4-pyrrolylphenyldiazonium salt [33, 51]. The presence of 4-pyrrolybenzene layer promoted the adhesion of polypyrrole chain on the substrates and the resulting film demonstrated improved anti-corrosion properties. Similarly, a thin layer of oligothiophene electroactive coating on glassy carbon, gold or platinum electrodes was realized through electroreduction of 2-aminoterthiophenyldiazonium followed by electropolymerization [52]. Recently, poly(3,4-ethylenedioxythiophene) (PEDOT) was covalently attached onto Pt/Ir electrodes through an intermediate phenylthiophene layer, deposited by electroreduction of the corresponding diazonium salt [53]. Resulting PEDOT films exhibited a very high adhesion stability, such that their electrochemical performances were retained after more than 1000 redox

cycles, whereas physically adsorbed PEDOT films begin to delaminate after 40 cycles. Polycarbazole and its derivatives are another important group of conducting polymers, which have been widely used in nanodevices, light emitting diodes, capacitators, rechargeable batteries, electrochemical transistors, or memory devices [54, 55]. However, the potentiality of a pre-grafted molecular film on the substrate surface by electroreduction of the corresponding aryldiazonium has not been previously investigated in improving the adhesion of polycarbazole layer on the substrate surface.

In this endeavour, the present work investigates the role of a molecular film of carbazole derivative, pre-grafted on a conducting ITO substrate by diazonium electroreduction, in improving the adhesion of different polycarbazole coatings. The key novelty aspect of this work is that a new carbazole derivative (9-methyl-9*H*-carbazole-3,6-diamine) is synthesized, which is subsequently electrografted on ITO surface through electroreduction of the corresponding diazonium salt. The electrografted surface has been comprehensively characterized by means of XPS, AFM, SEM and cyclic voltammetry to assess the molecular structure, surface morphologies and electroactivity. The molecular film coated on ITO is subsequently used as a functionalized substrate for the electropolymerization of different polycarbazole derivatives. The role of the carbazole molecular film is finally evaluated in improving the adhesion and long-term stability under water of different polycarbazole films.

2. Experimental

2.1.Materials and Reagents

All reagents and solvents used for the synthesis of 3,6-diamino-9-methylcarbazole were purchased from Sigma Aldrich and used as received without further purification. *9H*-Carbazole

(CAS: 86-74-8, purity ≥ 95%) and lithium perchlorate (CAS: 7791-03-9; purity ≥ 95%), sodium nitrite ($NaNO_2$) (CAS:7632-00-0; purity: 97%) and potassium hexacyanoferrate ($K_3[Fe(CN)_6]$) (CAS:13746-66-2; purity ≥ 99%), acetonitrile (CAS: 75-05-08, anhydrous, 99.8%) and potassium chloride (CAS: 7447-40-7; purity: 99%) were purchased from Sigma Aldrich. Indium Tin Oxide (ITO)-coated glass plates were purchased from Solems (12 ohms, ITO thickness: 370 nm, glass thickness: 1.1 mm, sheet sizes: 20 x 10 mm).

2.2.Electrochemical set up and methods

- Electrografting:

Cleaning of the ITO coated glass plates was performed in four steps before any electrochemical experiments. Indeed, they were sequentially cleaned with dichloromethane, acetone, ethanol and distilled water under ultrasonication for 10 minutes in each solvent. The electrodes were then dried under synthetic air flow. PGSTAT302N Autolab Metrohm potentiostat was used to conduct different electrochemical experiments associated to electrografting of m-Cz diamine. The instrument was equipped with Nova 2.1 software and a conventional 3-electrode set up, consisting of an ITO plate, a Saturated Calomel Electrode (SCE) and a Pt wire which were employed as working, reference and counter electrode, respectively.

The diazonium salt precursor was *in situ* synthesized in the electrochemical cell by mixing deoxygenated solutions of 2 mM of m-Cz diamine (in 0.1 M $LiClO_4$) with 0.1 M of $NaNO_{2(aq)}$ in the ratio of 12.5:1 (v/v). The reaction mixture was further bubbled with continuous argon flow for 10 minutes. The solution color changed to yellow, which is a characteristic feature of the formation of diazonium species. Electroreduction of m-Cz diazonium was performed by repetitive cyclic voltammetry (CV) cycles in the potential range of -0.2 to -0.75 V and with a scan rate of 40 mV s^{-1}. The film electrografted on ITO (m-Cz-ITO) was subsequently washed

in acetonitrile (ACN) solution and dried under ambient condition at room temperature. A CV was also recorded in 5 mM $K_3[Fe(CN)_6]$ in 0.1 M $KCl_{(aq.)}$ at a scan rate of 40 mV s^{-1}, using m-Cz-ITO electrode and bare ITO in the potential range of -0.2 to +0.6 V.

- Electropolymerization:

Electropolymerization of m-Cz diamine and Cz monomers was carried out at room temperature, using a SPELEC potentiostat/galvanostat, from Metrohm, in a conventional 3-electrode set up, consisting of an ITO plate, a SCE electrode and a Pt wire which were employed as working, reference and counter electrode, respectively. Electropolymerization of m-Cz diamine and Cz monomers, both 10 mM, was performed by repetitive CVs cycles in the potential range of 0 to +2 V and with a scan rate of 50 mV s^{-1} in 0.1 M $LiClO_4$ electrolytic solution of acetonitrile. The working electrode was rinsed with acetonitrile after each electrodeposition experiment. Then, the electrochemical activity of the electrodeposited polymer films was deduced from the cyclic voltammograms obtained at a bare or modified ITO electrode coated with a polymer film in 0.1 M $LiClO_4$ electrolytic solution of acetonitrile.

2.3.Surface characterizations

Elemental analysis and chemical structure determination of the m-Cz film electrografted on ITO and m-Cz diamine powder were conducted using a Versaprobe 5000 XPS spectrometer (ULVAC-PHI apparatus). For the measurements, a monochromatic and focused Al Kα X-ray source (1486.6 eV) was used. For each sample, a survey and core-level spectra of C1s, N1s and O1s were recorded over a spot size of 200 µm. To record the survey and core-level spectra, pass energies of 187.5 eV and 58.7 eV were used, respectively. AFM images of the m-Cz-ITO surface were recorded using a Bruker Icon-2 AFM instrument in nanoDMA peak-force tapping mode. A silicon probe (ScanAsyst, AIR-HR) with a spring constant: 0.4 N/m and tip radius of

2 nm was used to scan the surface. During the scan, peak-force frequency and amplitude were 2 kHz and in the range of 25–75 nm, respectively. Infrared spectra of the electrodeposited polymer films were obtained by Infrared Reflection Absorption Spectroscopy (IRRAS) in reflection geometry at a grazing-incidence angle of 65°. The infrared spectrometer used was a Vertex 70 FT-IR equipped with a DGTS detector. For each sample, 256 scans were recorded with a 2 cm^{-1} resolution. Water contact angles of the electrodeposited polymers were measured using a contact angle analyzer (Digidrop, from GBX) equipped with a CCD camera, a sample stage and a syringe holder. A 5 µL drop of ultrapure water was formed at the tip of a syringe needle and placed onto the sample surface by raising the sample until a contact was made. Then, an image of the drop was captured, and contact angles were determined by drawing the tangent close to the edge of the droplet. At least five drops were deposited on each electrodeposited film.

Surface morphology of each polycarbazole film was also investigated with a high-resolution Thermo Scientific Apreo 2 Scanning Electron Microscope (SEM) with an electron beam energy of 5 keV and a working distance of 10 mm. The thickness and roughness of the polycarbazole films were measured using a Dektak 150 surface profilometer. Both thickness and roughness were obtained by moving this stylus perpendicular to the film over a scan length of 2000 µm at a scan speed of 50 µm/s. 5 measurements were achieved at different positions for each polycarbazole film.

3. Results and discussion

3.1. Synthesis and characterizations of 9-methyl-*9H*-carbazole-3,6-diamine (m-Cz diamine)

Synthesis of the monomer was carried out in three steps starting from 9*H*-carbazole. By alkylation of 9*H*-carbazole with iodomethane in basic conditions, 9-methyl-9*H*-carbazole was

obtained in 88% yield (see Supporting information). Following this step, 9-methyl-9*H*-carbazole was nitrated using copper nitrate 2.5 hydrate. 9-Methyl-3,6-dinitro-9*H*-carbazole was isolated as an insoluble compound in 84% yield (see Supporting information). Finally, reduction of the nitro groups using hydrazine hydrate and palladium on charcoal enabled to isolate the targeted 9-methyl-9*H*-carbazole-3,6-diamine in 76% yield. The general strategy adopted for the synthesis of the monomer, the electrografting and the electropolymerization is summarized in Scheme 1. The characterization of the products is given in Supporting Information and consistent with the study from Kim *et al.* [56].

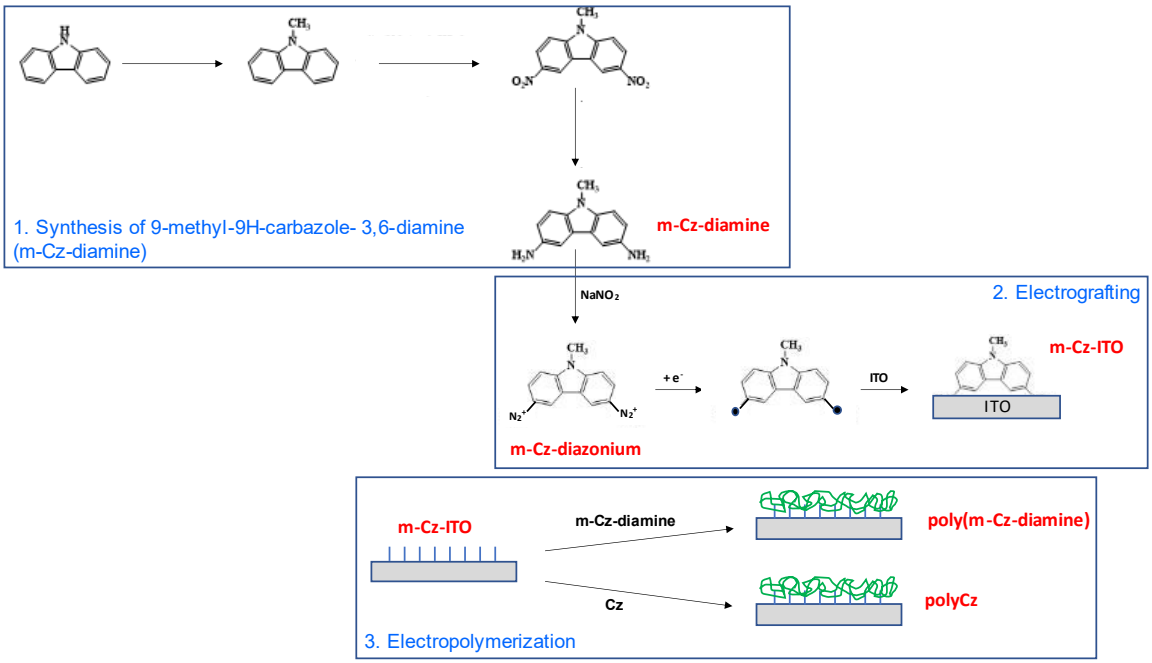

Scheme 1. General strategy adopted for the synthesis of the monomer, the electrografting and the electropolymerization of 9-methyl-9*H*-carbazole-3,6-diamine and carbazole.

3.2.Functionalization of ITO surface with carbazole derivative

Electrografting of m-Cz on ITO was realized by performing 40 CV cycles in the range of -0.2 V to -0.75 V in 0.1 M $LiClO_4$ electrolytic solution of ACN, containing 2 mM of precursor m-Cz diazonium. The voltammograms depicted in Fig. 1a exhibit an irreversible reduction

wave around -0.5 V, which is associated to electroreduction of m-Cz diazonium into m-Cz free radical, which is subsequently grafted on the electrode conducting surface. The grafting of the molecular film of m-Cz on the ITO surface is validated by the progressive decrease in the electroreduction current as a function of increasing CV cycles as highlighted in Fig. 1a. Such decrease in the electroreduction current is attributed to the coverage of ITO surface with a passivating organic film, which limits the access of m-Cz diazonium cation to the electrified ITO surface and thus decreases the electron transfer process. Notably, the major portion of the ITO surface is covered only within a few CV cycles, as electroreduction current decrease is very fast in the starting cycles. Subsequently, the electron transfer process is very slow and after 30 cycles the voltammograms are approximately superimposed to each other, confirming that the surface is almost completely covered with a passivating organic film. The presence of the electrografted layer can also be demonstrated by water contact angle measurements since the measured average water contact angle of bare ITO is 65° while electrografted ITO has an average water contact angle of 35°. A CV of the electrografted ITO electrode was also performed in $LiClO_4$ 0.1 M + acetonitrile to determine if the electrografted layer was electrochemically active (Fig. S6). The absence of oxidation peak on this CV indicated that the thin electrografted layer is not electroactive, just like poly(m-Cz diamine) films and unlike polyCz films (Fig. 5 and Fig. 8).

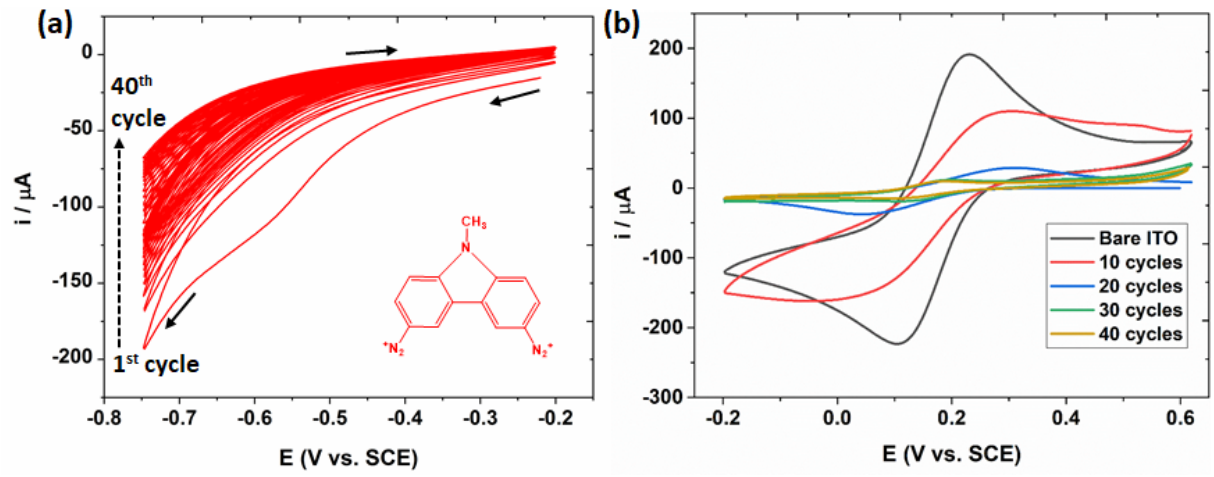

Figure 1: Voltammograms (40 cycles) of ITO-coated glass electrode recorded in 0.1 M $LiClO_4$ in ACN + 2 mM 9-methyl-*9H*-carbazole diazonium in a potential window of -0.2 V to -0.75 V at a scan rate of 40 mV s^{-1} (a). Comparison of CVs of 9-methyl-*9H*-carbazole grafted on ITO electrodes at different cycles and bare ITO electrode in 0.1 M KCl + 5 mM $K_3[Fe(CN)_6]$ at scan rate of 40 mV s^{-1}(b).

The surface coverage of ITO and passivating properties of m-Cz film was further evaluated by comparing the electroactivity of bare ITO and electrografted ITO surfaces towards redox process of $K_3[Fe(CN)_6]$ in aqueous medium. The comparison of the CVs as shown in Fig. 1b exhibits different redox profiles of $K_3[Fe(CN)_6]$ on different surfaces. On bare ITO electrode, a well-defined, sharp and reversible oxidation and reduction waves of $K_3[Fe(CN)_6]$ redox process is observed, indicating that bare ITO is easily accessible to redox probe hexacyanoferrate to exchange electrons for its redox reactions. However, redox current intensities decrease and peaks become broader on the m-Cz-ITO electrodes, confirming that electroactive surface of ITO is getting covered by a low conducting organic film. Moreover, the surface blocking effect of the m-Cz film electrografted on ITO is proportional to the number of CV cycles used in the electrografting process. Accordingly, surface blocking efficiency of the m-Cz film increases with the number of CV cycles used for its coating. Surface blockage

efficiency of each coating can be quantitatively assessed by equation (1), in which i_p*grafted* and i_p*bare* are the oxidation or reduction current of $K_3[Fe(CN)_6]$ redox process on a bare and m-Cz electrografted ITO electrodes, respectively.

$$Blockage\ efficiency = \left[1 - \frac{i_p grafted}{i_p bare}\right] \times 100 \text{ (equation 1)}$$

Based on this equation the blockage efficiency was estimated to 48.1%, 85.6%, 92.2% and 93.2% for the m-Cz films prepared by 10, 20, 30 and 40 CV cycles, respectively. Therefore, most of the surface passivation takes place in the initial CV cycles of the electrografting and reaches a saturation after 30 cycles, which is also evident in the pattern of electroreduction current decrease in Fig. 1a. Notably, the ITO surface blockage by m-Cz film does not reach 100%, which may be attributed to the presence of pinhole type defects [57], through which redox probe $[Fe(CN)_6]^{3+}$ can permeate and access the electrified ITO electrode for the electron transfer reaction.

3.3.Structural and topography characterizations of the electrografted film

The elemental composition and nature of chemical bond in the electrografted film were investigated by X-ray Photoelectron Spectroscopy. Figure 2 depicts the comparison of survey XPS spectra of the m-Cz film electrografted on ITO and the powder of m-Cz diamine, exhibiting the characteristic peaks associated to carbon, nitrogen and oxygen at ca. 285 eV, 399 eV and 531 eV, respectively. Notably, the relative peak intensity of O1s increases, while that of N1s decreases in the electrografted film spectrum, compared to the powder spectrum. The higher intensity of the O1s peak is attributed to the presence of oxygenated functionalities on the surface and bulk of the ITO substrate. On the other hand, decrease in the N1s intensity can be assigned to the removal of two amine functionalities as a consequence of diazotization reaction and subsequent covalent grafting on the surface, which is otherwise present in the precursor powder. The percentage of each of the elements was quantitatively assessed and is

given in Table S1. From the table, it is evident that oxygen content in the electrografted film increased to 42.5%, while nitrogen content decreased to 4.7%, compared to the precursor powder elemental composition, which also corroborates the observations in Fig. 2.

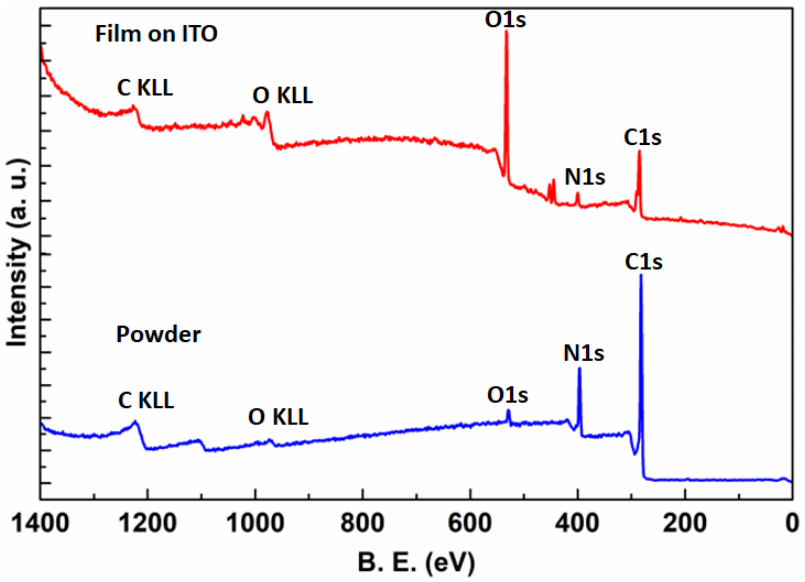

Figure 2: Comparison of XPS survey spectra of m-Cz film electrografted on ITO and m-Cz diamine powder.

The chemical structure of electrografted film was ascertained by analysing the core-level XPS spectra of C1s, N1s and O1s (Figure 3). The respective spectra of the precursor powder were also recorded as a control experiment. The deconvolution of C1s spectra reveals common peaks at ca. 284.5 eV and 286 eV for m-Cz diamine and m-Cz film electrografted on the ITO, which are characteristics to sp^2 C-C linkages [58] and C-N bonds. These features are expected in m-Cz film and m-Cz diamine molecules, owing to their π-conjugated structure and presence of aromatic amine moieties. Notably, the relative area under the curve peaking at 286 eV is higher in the electrografted film, which is attributed to the contribution from C-O bond formed between m-Cz molecule and ITO substrate. It also confirms the covalent grafting of m-Cz molecule on the ITO surface, leading to the formation of a molecular film. This assumption is

further validated by comparing the O1s spectra of electrografted film and the bare ITO (Fig. S7), depicting a common peak at ca. 530.2 eV associated to In-O bond in the bulk of ITO, while a contribution arising from surface hydroxide/oxy-hydroxide in bare ITO disappears in the spectrum of m-Cz-ITO. It indicates that the m-Cz molecule is linked to the ITO surface through its oxygenated functionalities on the surface (hydroxide/oxy-hydroxide) by a deprotonation reaction. Indeed, in the previous literature, it was reported that the linkage of organic molecules on ITO surface in aryldiazonium functionalization takes place through surface hydroxide/oxy-hydroxide groups of ITO [59]. The additional peak at ca. 289 eV in the C1s spectra can have multiple origins. At first, it can be assigned to the methyl group linked to pyrrolic nitrogen [60], which is expected in the powder as well as in the electrografted film. Moreover, larger area of the deconvoluted component in the spectra of electrografted film is ascribed to the nitrile group of ACN [61], which was used as a solvent in the electrografting process, that may remain adsorbed into the film.

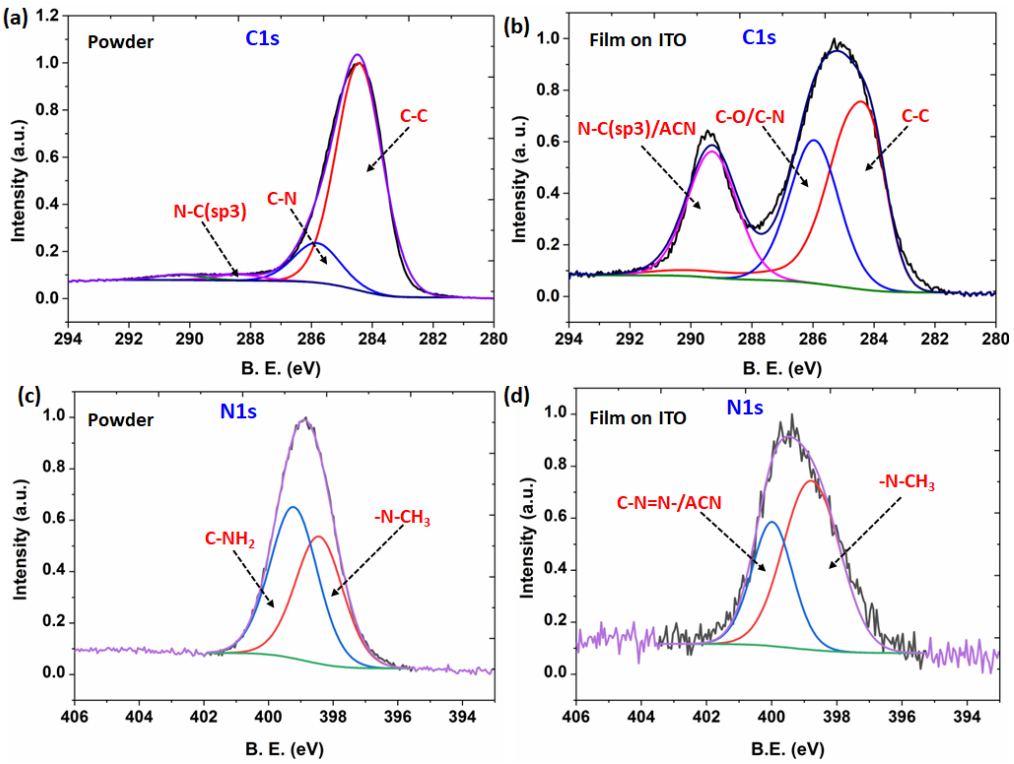

Figure 3: C1s spectra (a and b) and N1s spectra (c and d), and their deconvolution into different components for m-Cz diamine powder and m-Cz film electrografted on ITO substrate.

Since nitrogen containing functionalities are changing after the electrografting of m-Cz diamine on ITO surface, N1s spectra of the electrografted film and the precursor powder were investigated. The fitting and deconvolution of N1s spectrum of m-Cz diamine presents two peaks at 399.2 eV and 398.5 eV (Fig. 3c). In these two peaks, the former can be assigned to the aromatic amine group, while the latter is associated to pyrrolic nitrogen (N-CH_3) [62, 63]. Notably, the area of the curve attributed to amine-nitrogen is larger than the curve linked to pyrrol-nitrogen, which is consistent with the presence of two amine groups and one N-CH_3 group in the molecule. Electrografting is accompanied by the loss of two aromatic amine groups of m-Cz diamine, leading to a significant decrease of nitrogen content in the electrografted film. Accordingly, N1s spectrum of the electrografted film presents very noisy signals as depicted in Fig. 3d. The fitting of the experimental spectrum reveals two components, in which the one at lower energy is attributed to N-CH_3 functionality of the electrografted molecule as observed in the precursor compound, while the other at higher energy (ca. 400 eV) can have different origins, such as azo compounds and nitrile group of the adsorbed solvent species in the film [64, 65]. The formation of azo-compounds was previously reported in aryldiazonium based surface functionalization, which arises because diazonium derivative may undergo electrophilic substitution reactions on the pre-grafted molecular layer [66].

SEM pictures of bare ITO and electrografted ITO surfaces were performed to compare their topography (Fig. S8). It appears that the topography of the two surfaces is very similar so that the electrografted layer does not really modify the topography of the initial substrate. After that, the topography of the electrografted ITO was also investigated by AFM imaging, which is depicted in Fig. 4. From the images, it is evident that the surface of the m-Cz-ITO surface has

two different topographical features, consisting of a smooth region, over which oval shape grains are developed and are distributed non-homogeneously. The roughness (root mean square; rms) of the surface (in Fig. 4a) can be estimated to ca. 95 nm. The magnified image in Fig. 4b clearly reveals the shape of the grains, exhibiting the assembly of two or more than two oval shaped grains at different nucleation sites. For the selected linescan, the height of the grains varies between ca. 150 nm and 200 nm (Fig. 4c), while their width is ca. 300 nm. The other region corresponds to a smooth topography, which surface height variation is depicted in Fig. 4d through the linescan represented in Fig. 4b. It is clear from the linescan that surface height changes only by a few nm on the smooth region. The rms (root mean square) roughness of the smooth region was estimated to ca. 4.3 nm.

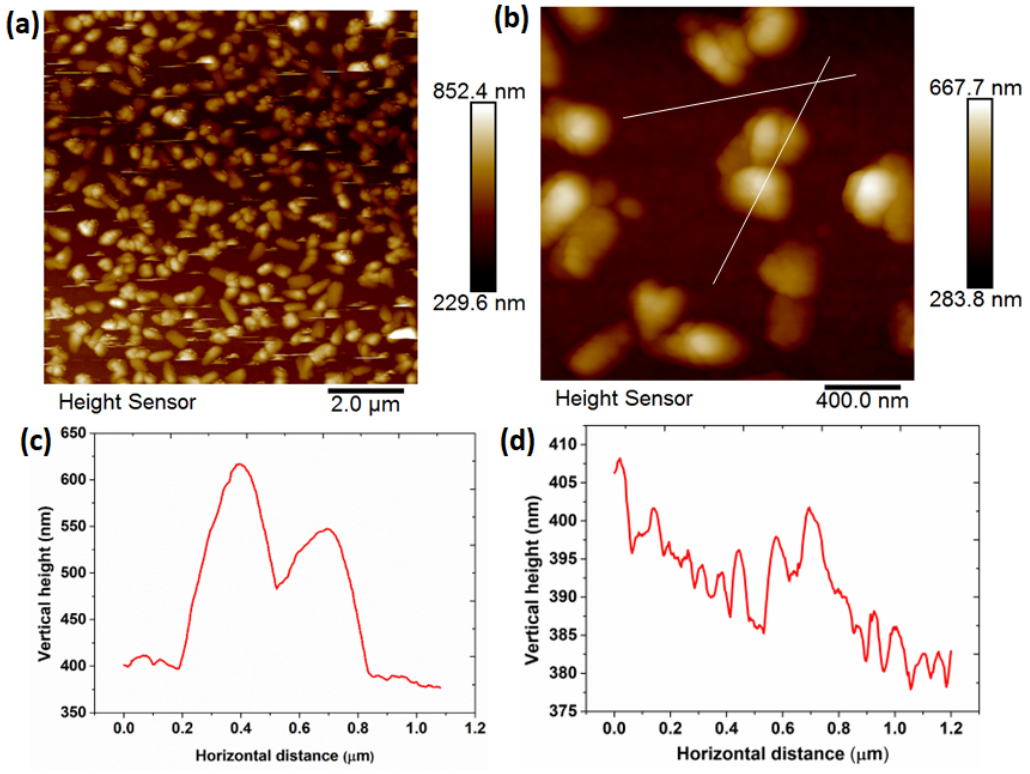

Figure 4: AFM images (a and b) and surface height variations (c and d) of m-Cz-ITO surface.

3.4.Electrodeposition and characterization of poly(3,6-diamino-9-methylcarbazole) on bare and modified ITO

Electrochemical oxidation of 9-methyl-9*H*-carbazole-3,6-diamine was carried out by cyclic voltammetry in a potential range of 0 to +2 V/SCE at a bare ITO electrode and at the functionalized ITO electrode. The corresponding voltammograms are depicted in Fig. 5. During the first scan, two anodic peaks, due to the oxidation of the m-Cz diamine monomers into radical cations at the bare ITO, appear at +0.3 and +1.2 V/SCE (Fig. 5a). After the first scan, the oxidation peaks decrease gradually and become less and less distinguishable. If the presence of a grey film attests to the electrochemical deposition of a substituted polycarbazole film of poly(m-Cz diamine) on the bare ITO surface, the gradual decrease of the oxidation peak intensity with repeated scans indicates that this polymer film is not very conducting. Moreover, no redox process associated with poly(m-Cz diamine) is observed, unlike what is generally obtained for other organic polymers prepared by anodic oxidation such as polypyrrole, PEDOT, polyaniline or polycarbazole [67-70]. To confirm the lack of electrochemical activity of the electrodeposited films, the electrode with the poly(m-Cz diamine) film attached is removed from the growth electrolytic solution and placed in a monomer-free solution of acetonitrile + 0.1 M $LiClO_4$ for post-polymerization voltammetric analysis. Since the resulting post-polymerization CV has no significant reduction peak and the intensity of the oxidation peak is low and gradually decreases, it can be concluded that these polymer films are not very electroactive (Fig 5c).

To check that the films obtained on bare ITO and electrografted ITO have the same chemical structure, infrared spectra of the poly(m-Cz-diamine) films were performed (Fig. S9). The spectra appeared very similar and contained the characteristic vibration bands of carbazole compounds [71]. These vibration bands correspond to the stretching vibration of primary amino bonds at 3200-3400 cm^{-1}, stretching vibration of aromatic C-H bonds at 3050 cm^{-1}, stretching vibration of aliphatic C-H bonds at 2950 cm^{-1}, aromatic stretching of double bond C=C and single bond C-C at 1600 cm^{-1} and 1500 cm^{-1}, valence vibration of C-N bond of carbazole cycle

at 1300 cm^{-1}, and in plane deformation of the C-H bonds of the phenyl ring at 1100 cm^{-1}. The vibration band at 3600 cm^{-1} is not characteristic of the deposited film but is probably due to the presence of hydroxyl bonds on the surface of the ITO substrate.

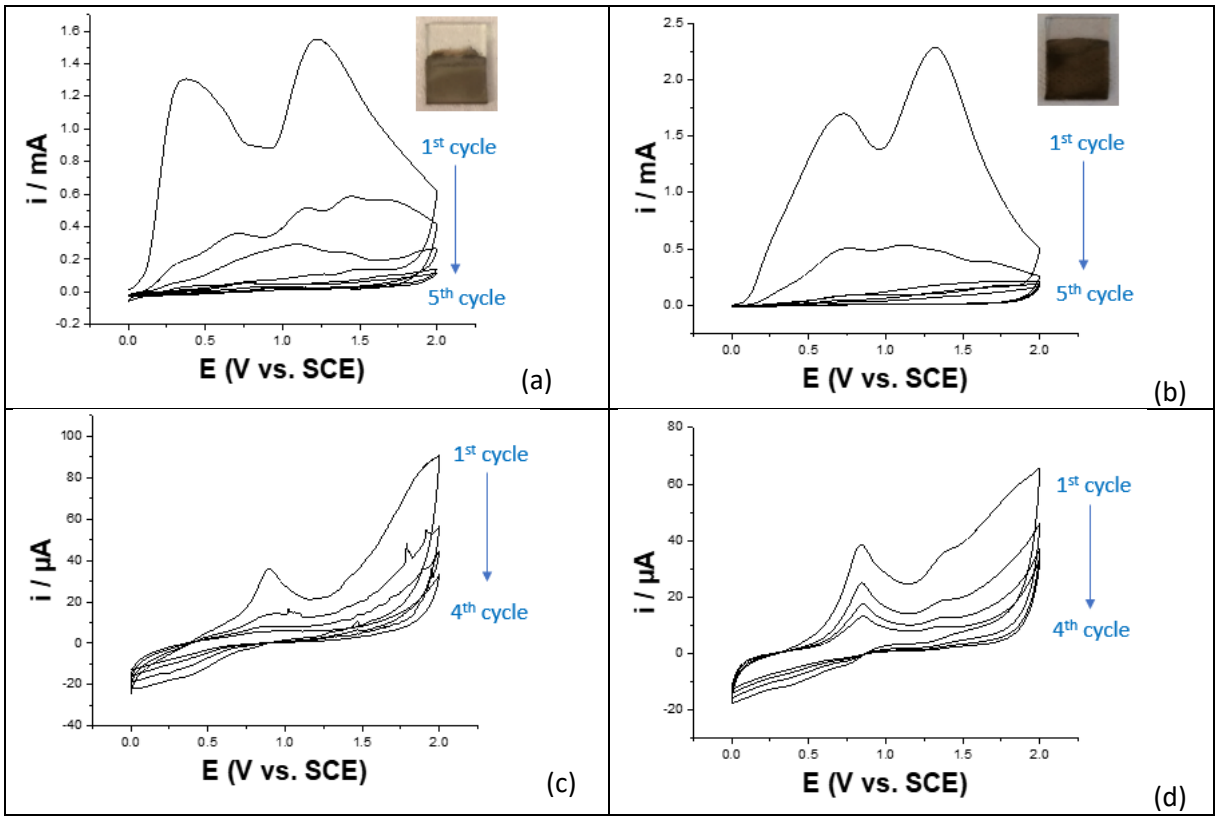

Figure 5: Electrochemical oxidation of 9-methyl-9*H*-carbazole-3,6-diamine (0.01 M) in acetonitrile + 0.1 M $LiClO_4$: (a) on bare ITO, (b) on m-Cz-ITO. Post-polymerization cyclic voltammetry of the resulting films in acetonitrile + 0.1 M $LiClO_4$: (c) on bare ITO, (d) on m-Cz-ITO.

The same experiments are then carried out on electrodes previously electrografted with m-Cz film. The cyclic voltammetry obtained on the electrografted ITO is very similar to that obtained on bare ITO (Fig 5b). It can just be noticed that the current is slightly higher during the first cycle but decreases a little faster during the following cycles. In addition, the film does not appear electroactive even if the current observed on the post-polymerization CVs has slightly higher intensities than on bare ITO (Fig 5d). The resulting film is also grey but slightly

darker. The profilometric measurements show that both films obtained by electropolymerization have quite similar thicknesses since thicknesses of 133 nm and 117 nm are found for films electrodeposited on bare ITO and m-Cz-ITO, respectively. On the contrary, polymer films electrodeposited on m-Cz-ITO appear smoother since the average roughness is 7 nm compared to 18 nm for films electrodeposited on bare ITO. The low thickness of poly(m-Cz diamine) films, compared to usual conducting polymer films, such as polycarbazole, electrodeposited under the same conditions (see section 3.4.), is probably due to the lower conductivity of the films as indicated by cyclic voltammetry. SEM images of electroplated poly(m-Cz diamine)films on bare ITO and m-Cz-ITO are given Figure 6. It is apparent that (i) the structure of polymer films is very different from the structure of electrografted layers previously observed (Figure S8), (ii) the structure of polymer films is similar whether or not the ITO substrate has been coated with an electrografted layer, (iii) the polymer film fully covers the surface but does not have the usual granular structure of conducting polymer films such as polycarbazole (see section 3.4.).

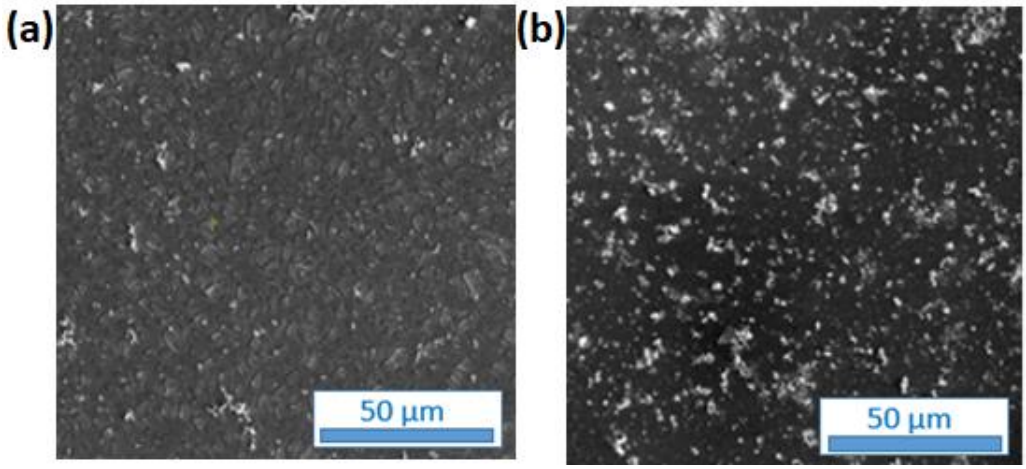

Figure 6: SEM images of the poly(m-Cz diamine) films electrodeposited on bare ITO (a) and m-Cz-ITO (b) surfaces.

The adhesion of a poly(m-Cz diamine)film to a bare ITO surface and to an electrografted ITO surface was then compared. First, the adhesion of the polymer films to the substrate was tested with a very sticky tape (Figure 7a), then the polymer films were immersed in water for 2 months before being removed and observed (Fig 7b). As can be seen in Figure 7, the test with scotch tape is successful for both substrates since very little material is found on the scotch tape both on the bare ITO and m-Cz-ITO substrates coated with poly(m-Cz diamine). Therefore, in air, the electrografted layer does not appear to improve the adhesion of the polymer to the substrate. However, after prolonged immersion in water, the poly(m-Cz diamine)film remains well attached to the substrate coated by reduction of the diazonium and polymer, whereas this is not the case for the substrate without electrografted layer. In a liquid environment, there is therefore an improvement in adhesion thanks to diazonium pathway.

Figure 7: Adhesion test with a scotch tape of a poly(m-Cz diamine)film electrodeposited on bare ITO (a) and m-Cz-ITO (b). (c): Left: picture of the film (a) after immersion in water for 2 months, right: picture of the film (b) after immersion in water for 2 months.

3.5.Electrodeposition, characterization and adhesion of polycarbazole on bare and modified ITO

To test the influence of the layer obtained by reduction of the diazonium on the properties of a more conductive and more conventional polymer, the previous experiments were

reproduced using carbazole monomers instead of 9-methyl-9*H*-carbazole-3,6-diamine monomers. Thus, the electrochemical oxidation of carbazole (10 mM) is first performed by cyclic voltammetry at a bare ITO electrode in 0.1 M $LiClO_4$ electrolytic solution of acetonitrile (Fig. 8a). During the first scan, an anodic peak, due to the oxidation of the monomers into radical cations, appears at +1.6 V/SCE. After the first scan, the intensity of the oxidation potential increases and then decreases gradually while the oxidation potential also tends to decrease. The appearance of a black film on the ITO electrode during the electrochemical deposition indicates the formation of a polycarbazole film (polyCz). Moreover, there is a peak of reduction at +0.6 V/SCE and a peak of oxidation at +0.8 V/SCE which both increase with the cycles and correspond to redox peaks due to the reduction/oxidation of polycarbazole films as they grow. Post-polymerization voltametric analyses were then performed to confirm the electrochemical activity of the electrodeposited polyCz films (Figure 8c). The resulting CV showed that the redox process of polyCz takes place since a significant oxidation peak is visible at +1.4 V/SCE and a significant reduction peak at +0.8 V/SCE. Moreover, the intensities of oxidation and reduction processes are quite similar indicating that a similar amount of polymer is involved in the oxidation and in the reduction process. Besides, the intensity of these peaks gradually decreases with successive cycles indicating that the doping of the polyCz films by the perchlorate anions becomes more and more difficult with successive cycles. To determine the influence of the adhesion tests on the electroactivity of the polyCz films, the same electrochemical experiments were performed after the adhesion tests, which led to the conclusion that the electroactivity was not affected by the adhesion tests since the same oxidation and reduction peaks were present on the resulting CV. Only a small decrease in the intensity of the anodic and cathodic peaks was observed (less than 10% of the intensity measured before the adhesion tests).

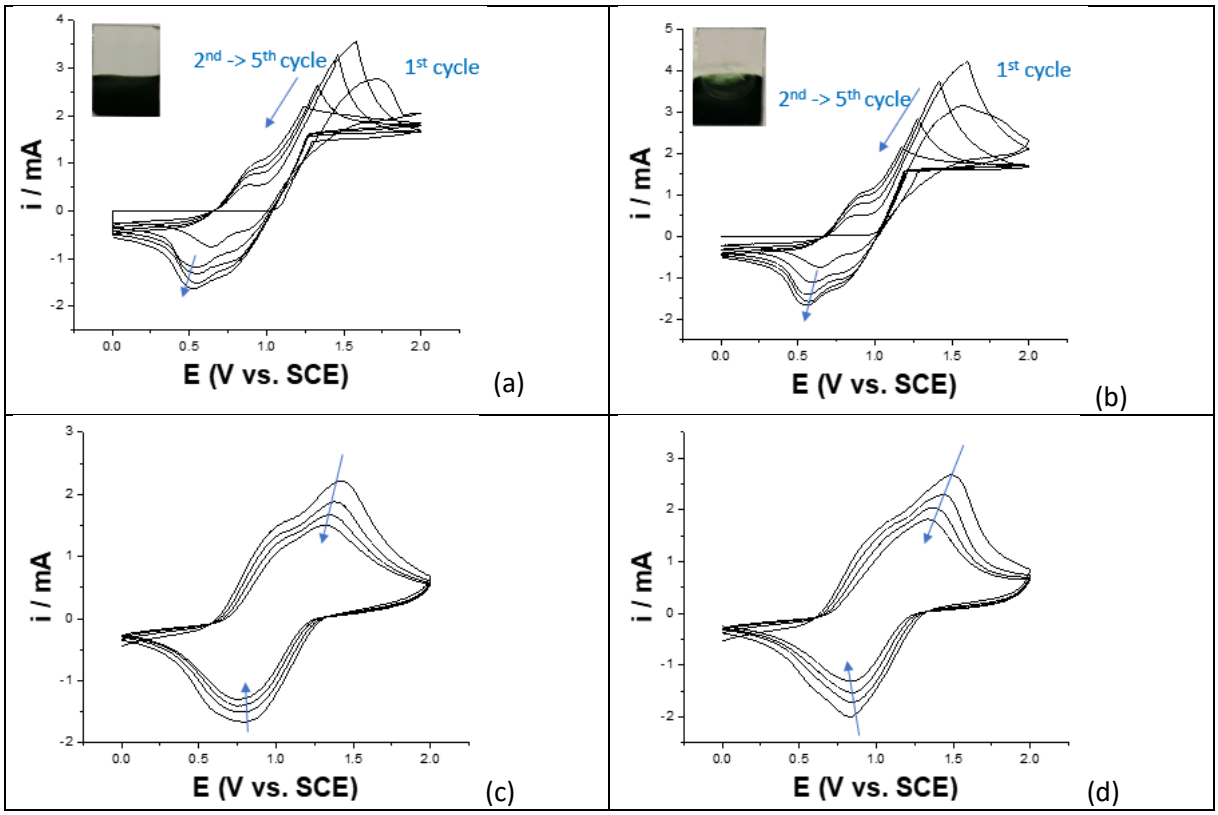

Figure 8: Electrochemical oxidation of carbazole monomers (0.01 M) in acetonitrile + 0.1 M $LiClO_4$: (a) on bare ITO, (b) on m-Cz-ITO. Post-polymerization cyclic voltammetry of the resulting films in acetonitrile + 0.1 M $LiClO_4$: (c) on bare ITO, (d) on m-Cz--ITO.

The same experiments were then performed on ITO electrodes previously electrografted by reduction of carbazole diazonium. The resulting cyclic voltammogramms (Fig 8b) are quite similar to that obtained on the bare ITO. Indeed, the oxidation/reduction peaks appear at the same potentials and the evolution of the current intensity with successive cycles is quite identical. Similarly, the electrochemical activity of electrodeposited polyCz films is not affected by the presence of the electrografted layer on the surface of the ITO electrode since there is also a high electrochemical activity with pronounced oxidation and reduction peaks characteristic of the phenomenon of doping/dedoping of the polymer film by perchlorate anions. (Fig 8d). Whether the ITO surface is coated with a layer obtained by reduction of a diazonium or not, the electrodeposited polymer film is black. Profilometric measurements show that the films

obtained by electropolymerization have a thickness of a few micrometers (4.7 µm for films electrodeposited on bare ITO and 3.0 µm for those electrodeposited on m-Cz-ITO). The difference in thickness does not come from a different current intensity during electropolymerization but could possibly come from a lower efficiency of the electropolymerization reaction due to the presence of the electrografted layer on the ITO electrode. In addition, polymer films electrodeposited on m-Cz-ITO appear slightly smoother since their average roughness is 1.3 µm against 1.7 µm for films electrodeposited on bare ITO. The morphology of polyCz films electrodeposited on bare ITO and m-Cz-ITO was studied by SEM microscopy (Figure 9). The SEM images indicate that the entire surface of the polyCz film is homogeneous. Moreover, both substrates are almost completely covered by the polymer films which consist of micrometer circular globules aggregated to each other. As for the poly(m-Cz diamine) film, the IR spectra of the polyCz films deposited on bare ITO and electrografted ITO led to similar spectra showing the characteristic vibrational bands of carbazole compounds (stretching vibration of N-H bonds at 3500 cm^{-1}, stretching vibration of aromatic C-H bonds at 3050 cm^{-1}, stretching vibration of aliphatic C-H bonds at 2950 cm^{-1}, aromatic stretching of double bond C=C and single bond C-C at 1650 cm^{-1} and 1500 cm^{-1}, valence vibration of C-N bond of carbazole cycle at 1250 cm^{-1}, and in plane deformation of the C-H bonds of the phenyl ring at 1050 cm^{-1}).

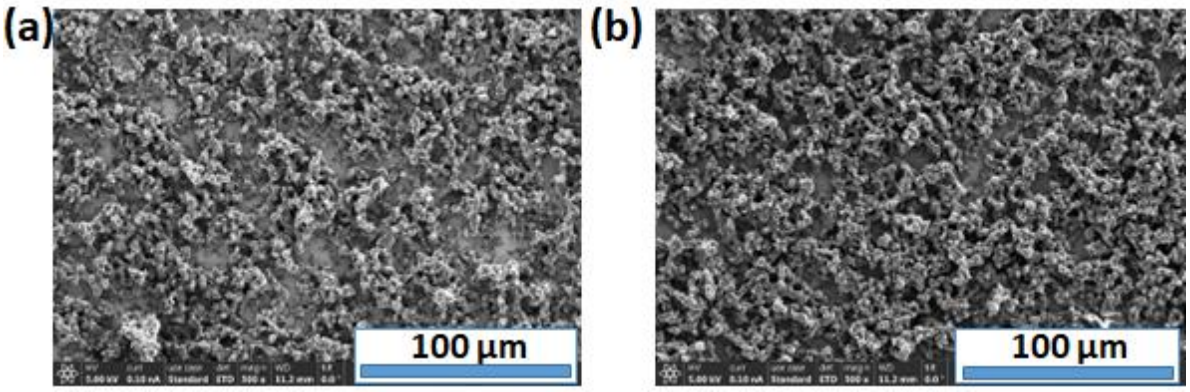

Figure 9: SEM images of the polyCz films electrodeposited on bare ITO (a) and m-Cz-ITO (b) surfaces.

The adhesion of the polyCz film to a bare ITO surface (Fig. 10a) and to an electrografted ITO surface (Fig. 10b) is then compared using the sticky tape. This test is successful for the electrografted ITO, even if a small portion of the polyCz film remains on the tape. On the contrary, the test is not successful for the bare ITO since a large part of the polyCz film remains on the tape. Therefore, in air, the electrografted layer seems to improve the adhesion of the polymer to the substrate. Then, the polymer films electrodeposited on bare ITO and electrografted ITO were immersed in a Fisher Scientif S line ultrasonic cellular (frequency: 37 kHz, US power: 90 W) for 60 min. No degradation was observed on the film after this US treatment. After that, the polymer films were immersed in water for 2 months before being removed and observed (Figure 10c). This prolonged immersion in water causes a very large portion of the polyCz film deposited on bare ITO to detach, while that deposited on electrografted ITO remains attached. The electrografted layer thus allows a significant improvement of the adhesion of the polyCz film to the substrate in water, which is important for potential applications as (bio)sensors in aqueous solutions for example. The results obtained in this study are comparable with those obtained by Jacques *et al.* [33] and Lo *et al.* [72] who both studied the adhesion enhancement of a polymer film on an electrografted layer. Thus, the electropolymerization of pyrrole was achieved on Ni and NiTi alloy substrates, which were pre-grafted with 4-pyrrolylbenzene via electroreduction of 4-pyrrolylphenyldiazonium salt. Peeling tests, which consisted of scratching the modified sample with a metallic comb and then stacking a scotch-tape on the scraped sample before removing the scotch-tape from the modified-surface, were successfully performed to evaluate the adhesion of the electrodeposited polymers [33]. Similarly, polypyrrole films were electrodeposited on aminobenzenediazonium-modified ITO in aqueous media [72]. Without diazonium pretreatment, the polypyrrole film delaminated

readily upon sonication or during ultrahigh vacuum outgassing prior to XPS analysis. In contrast, a pretreatment involving electrografting of a diazonium layer resulted in excellent adhesion of polypyrrole, which withstood 75 min of ultrasonication and allowed the use of these modified electrodes for the detection of lead (II) ions.

Figure 10: Adhesion test with a scotch tape of a polyCz film electrodeposited on bare ITO (a) and m-Cz-ITO (b). Picture of the same films after immersion in water for 2 months (c).

4. Conclusion

In this work, a molecule of 9-methyl-9*H*-carbazole-3,6-diamine was synthesized and covalently grafted onto an ITO surface to confer strong adhesion to polycarbazole films electrodeposited on the so-functionalized surface. Functionalization of the ITO surface was achieved by diazonium electroreduction, generating an electrochemically passive organic coating. Elemental analysis and chemical structure investigation by XPS confirmed the covalent bonding of m-Cz on ITO through its surface oxygen functionalities. The surface of the functionalized ITO revealed a rough topography in which submicrometer oval grains of m-Cz are inhomogeneously distributed on the electrografted film. These surface features were also confirmed by SEM morphological studies. The oxidative electropolymerization of m-Cz and Cz on the functionalized ITO surface revealed a strong improvement in the adhesion of the polymers chain, compared to the similar electropolymerization performed on the bare ITO surface. Indeed, the stability tests performed by scotch tape and immersion under water for 2 months showed a high robustness of the polymer films deposited on the functionalized ITO

which remain intact on the surface. In contrast, the polymer films deposited on the bare ITO surface showed poor adhesion and are removed from surface. Thus, it is clearly demonstrated that functionalization of the ITO surface with m-Cz promotes the adhesion of polymer films without altering their electrochemical properties. The high stability of the polymer coatings in air and liquid environments, conferred by diazonium electroreduction functionalization, appears promising for applications as a protective membrane.

Acknowledgments:

This research was funded by the European Union through the Fonds Européen de Développement Régional (FEDER), and the Regional Council of Bourgogne Franche-Comté through both the PIA-excellence ISITE-BFC program CoMICS: Chemistry of Molecular Interactions Catalysis and Sensors and the Envergure Program MatElectroCap. A. K. acknowledges financial support from BQR program (Université de Bourgogne).

Author Contributions:

Methodology, B.L.; investigation, F.D., A.K., S.L., E.C.; writing—review and editing, M.B., R.M.P., A.K., B.L., L.V.; funding acquisition, M.B, L.V. All authors have read and agreed to the published version of the manuscript.

5. References

[1] H. Letheby, XXIX. On the production of a blue substance by the electrolysis of sulphate of aniline, J. Chem. Soc. 15 (1862) 161-163. https://doi.org/10.1039/JS8621500161.

[2] H. Shirakawa, E.J. Louis, A.G. MacDiarmid, C. K. Chiang, A. J. Heeger, Synthesis of electrically conducting organic polymers: halogen derivatives of polyacetylene, (CH)x**,** J. Chem. Soc., Chem. Commun. (1977) 578-580. https://doi.org/10.1039/C39770000578.

[3] A.F. Diaz, K.K. Kanazawa, G.P. Gardini, Electrochemical polymerization of pyrrole, J. Chem. Soc., Chem. Commun. (1979) 635-636. https://doi.org/10.1039/c39790000635.

[4] G. Tourillon, F.J. Garnier, New electrochemically generated organic conducting polymers, Electroanal. Chem. 135 (1982) 173-178. https://doi.org/10.1016/0022-0728(82)90015-8.

[5] A.A. Correa, E.C. Pereira, A.J.A. de Oliveira, Magnetic Properties of Conducting Polymers. In: La Porta, F., Taft, C. (eds) Emerging Research in Science and Engineering Based on Advanced Experimental and Computational Strategies. Engineering Materials. Springer, Cham. 2020. https://doi.org/10.1007/978-3-030-31403-3_19.

[6] K. Namsheer, C.S. Rout, Conducting polymers: a comprehensive review on recent advances in synthesis, properties and applications, RSC Adv. 11 (2021) 5659-5697. https://doi.org/10.1039/d0ra07800j.

[7] F.G. Zamani, H. Moulahoum, M. Ak, D.O. Demirkol, S. Timur, Current trends in the development of conducting polymers-based biosensors, TrAC 118 (2019) 264-276. https://doi.org/10.1016/j.trac.2019.05.031.

[8] Y.C. Wong, B.C. Ang, A.S.M.A. Haseeb, A.A. Baharuddin, Y.H. Wong, Conducting polymers as chemiresistive gas sensing materials: a review, J. Electrochem. Soc. 167 (2019) 037503. https://doi.org/10.1149/2.0032003JES.

[9] M. Tessarolo, I. Gualandi, B. Fraboni, Recent progress in wearable fully textile chemical sensors, Adv. Mater. Tech. 3 (2018) 1700310. https://doi.org/10.1002/admt.201700310.

[10] B. Lakard, Electrochemical biosensors based on conducting polymers: A review, Appl. Sci. 10 (2020) 6614. https://doi.org/10.3390/app10186614.

[11] Y. Han, L. Dai, Conducting polymers for flexible supercapacitors, Macromol. Chem. Phys. 220 (2019) 1800355. https://doi.org/10.1002/macp.201800355.

[12] S. Ramanavicius, A. Ramanavicius, Conducting polymers in the design of biosensors and biofuel cells, Polymers 13 (2020) 49. https://doi.org/10.3390/polym13010049.

[13] Y. Chen, S. Zhuo, Z. Li, C. Wang, C, Redox polymers for rechargeable metal-ion batteries EnergyChem. 2 (2020) 100030. https://doi.org/10.1016/j.enchem.2020.100030.

[14] A.R. Murad, A. Iraqi, S.B. Aziz, S.N. Abdullah, M.A. Brza, Conducting polymers for optoelectronic devices and organic solar cells: A review, Polymers 12 (2020) 2627. https://doi.org/10.3390/polym12112627.

[15] T.A. Kung, N.B. Langhals, D.C. Martin, P.J. Johnson, P.S. Cederna, M.G. Urbanchek, Regenerative peripheral nerve interface viability and signal transduction with an implanted electrode, Plast. Reconstr. Surg. 133 (2014) 1380-1394. https://doi.org/10.1097/PRS.0000000000000168.

[16] C.M. Frost, B. Wei, Z. Baghmanli, P.S. Cederna, M.G. Urbanchek, PEDOT electrochemical polymerization improves electrode fidelity and sensitivity, Plast. Reconstr. Surg. 129 (2012) 933-942. https://doi.org/10.1097/PRS.0b013e31824422bf.

[17] M.R. Abidian, J.M. Corey, D.R. Kipke, D.C. Martin, Conducting-polymer nanotubes improve electrical properties, mechanical adhesion, neural attachment, and neurite outgrowth of neural electrodes, Small 6 (2010) 421-429. https://doi.org/10.1002/smll.200901868.

[18] T. Peng, W.W. Sun, C.L. Huang, W.J. Yu, B. Sebo, Z.G. Dai, S.S. Guo, X.Z. Zhao, Self-assembled free-standing polypyrrole nanotube membrane as an efficient FTO- and Pt-free counter electrode for dye-sensitized solar cells, ACS Appl. Mater. Interf. 6 (2014) 14–17. https://doi.org/10.1021/am404265q.

[19] S. Cui, J. Mao, M. Rouabhia, S. Elkoun, Z. Zhang, A biocompatible polypyrrole membrane for biomedical applications, RSC Advances 11 (2021), 16996-17006. https://doi.org/10.1039/d1ra01338f.

[20] E. Smela, Thiol-modified pyrrole monomers: 4. Electrochemical deposition of polypyrrole over 1-(2-thioethyl)pyrrole, Langmuir 14 (1998) 2996-3002. https://doi.org/10.1021/la970863e.

[21] L.F. Rozsnyai, M.S. Wrighton, Controlling the adhesion of conducting polymer films with patterned self-assembled monolayers, Chem. Mater. 8 (1996) 309-311. https://doi.org/10.1021/cm9502838.

[22] R.A. Simon, A.J. Ricco, M.S. Wrighton, Synthesis and characterization of a new surface derivatizing reagent to promote the adhesion of polypyrrole films to n-type silicon photoanodes: N-(3-(trimethoxysilyl)propyl)pyrrole, J. Am. Chem. Soc. 104 (1982) 2013-2034. https://doi.org/10.1021/ja00371a045.

[23] C.M. Sougueh, S. Lakard, J. Husson, E. Contal, S. Monney, V. Moutarlier, C. Magnenet, B. Lakard, Influence of pre-grafted pyrrole-based silane on the electrodeposition and chemical properties of polypyrrole films, Synth. Met. 246 (2018) 220-229. https://doi.org/10.1016/j.synthmet.2018.10.017.

[24] C. Peng, N. Cao, Z. Qi, Y. Yan, R. Wu, G. Wang. Preparation and Corrosion Performance of PPy/Silane Film on AZ31 Magnesium Alloy via One-Step Cyclic Voltammetry, Polymers 13 (2021) 3148. https://doi.org/10.3390/polym13183148.

[25] S. Bianchi, M. Trueba, S.P. Trasatti, E. Madaschi, M.C. Sala, An in-depth comprehension of the protection mechanism of Al alloys by aniline-based silane, Prog. Org. Coat. 77 (2014) 2054-2065. https://doi.org/10.1016/j.porgcoat.2014.02.005.

[26] N. Roosz, M. Euvrard, B. Lakard, L. Viau, A straightforward procedure for the synthesis of silica@ polyaniline core-shell nanoparticles, Coll. Surf. A 573 (2019) 237-245. https://doi.org/10.1016/j.colsurfa.2019.04.036.

[27] Y.Z. Dong, W.J. Han, H.J. Choi, Polyaniline coated core-shell typed stimuli-responsive microspheres and their electrorheology, Polymers 10 (2018) 299-331. https://doi.org/10.3390/polym10030299.

[28] M.M.P. Parel, I.R. Colambo, M.U. Herrera, Synthesis of polyaniline on functionalized TiO_2 using two-container type in situ coating technique, J. Coat. Tech. Res. 19 (2022) 851-857. https://doi.org/10.1007/s11998-021-00562-1.

[29] V.D. Hodoroaba, S. Rades, P. Borghetti, E. Ortel, T. Wirth, S. Garcia, E. Gomez, M. Blanco, G. Alberto, G. Martra, Organic surface modification and analysis of titania nanoparticles for self-assembly in multiple layers, Surf. Interf. Anal. (2020) 1-6. https://doi.org/10.1002/sia.6842.

[30] A. Mesnage, X. Lefèvre, P. Jegou, G. Deniau, S. Palacin, Spontaneous grafting of diazonium salts: chemical mechanism on metallic surfaces, Langmuir 28 (2012) 11767-11778. https://doi.org/10.1021/la3011103.

[31] A.A. Mohamed, Z. Salmi, S.A. Dahoumane, A. Mekki, B. Carbonnier, M.M. Chehimi, Functionalization of nanomaterials with aryldiazonium salts, Adv. Coll. Interf. Sci. 225 (2015) 16-36. https://doi.org/10.1016/j.cis.2015.07.011.

[32] Bui-Thi-Tuyet, V.; Cannizzo, C.; Legros, C.; Andrieux, M.; Chaussé, A. Modification of fluorine-doped tin oxide surface: Optimization of the electrochemical grafting of diazonium salt, Surf. Interf. 15 (2019) 110-116. https://doi.org/10.1016/j.surfin.2019.01.012.

[33] A. Jacques, S. Devillers, J. Delhalle, Z. Mekhalif, Electrografting of In Situ Generated Pyrrole Derivative Diazonium Salt for the Surface Modification of Nickel, Electrochim. Acta 109 (2013) 781-789. https://doi.org/10.1016/j.electacta.2013.07.178.

[34] A. Berisha, M.M. Chehimi, J. Pinson, F.I. Podvorica, Electrode surface modification using diazonium salts, Electroanal. Chem. 26 (2016) 115-225. https://doi.org/10.1016/j.electacta.2012.05.044.

[35] A. Kumar, R. Meunier-Prest, F. Herbst, O. Heintz, E. Lesniewska, M. Bouvet, Covalent grafting of aryls to modulate the electrical properties of phthalocyanine-based heterostructures: Application to ammonia sensing, Chem. Eng. J. 436 (2022) 135207. https://doi.org/10.1016/j.cej.2022.135207.

[36] P. Allongue, M. Delamar, B. Desbat, O. Fagebaume, R. Hitmi, J. Pinson, J.M. Saveant, Covalent modification of carbon surfaces by aryl radicals generated from the electrochemical reduction of diazonium salts, J. Am. Chem. Soc. 119 (1997) 201-207. https://doi.org/10.1021/ja963354s.

[37] J. Pinson, F. Podvorica, Attachment of organic layers to conductive or semi conductive surfaces by reduction of diazonium salts, Chem. Soc. Rev. 34 (2005) 429-439. https://doi.org/10.1039/b406228k.

[38] C. Gauthier, I. Lopez, T. Breton, A post-functionalization toolbox for diazonium (electro)-grafted surfaces: review of the coupling methods, Mater. Adv. 2 (2021) 2773-2810. https://doi.org/10.1039/d1ma00077b.

[39] D. Hetemi, V. Noël, J. Pinson, Grafting of Diazonium Salts on Surfaces: Application to Biosensors, Biosensors 10 (2020) 4. https://doi.org/10.3390/bios10010004.

[40] D. Li, Y. Luo, D. Onidas, L. He, M. Jin, F. Gazeau, J. Pinson, C. Mangeney, Surface functionalization of nanomaterials by aryl diazonium salts for biomedical sciences, Adv. Coll. Interf. Sci. 294 (2021) 102479. https://doi.org/10.1016/j.cis.2021.102479.

[41] P. Yáñez-Sedeño, S. Campuzano, J.M. Pingarrón, Integrated affinity biosensing platforms on screen-printed electrodes electrografted with diazonium salts, Sensors 18 (2018) 675. https://doi.org/10.3390/s18020675.

[42] C. Ott, M.D. Raicopol, C. Andronescu, E. Vasile, A. Hanganu, A. Pruna, L. Pilan, Functionalized polypyrrole/sulfonated graphene nanocomposites: Improved biosensing platforms through aryl diazonium electrochemistry, Synth. Met. 235 (2018) 20-28. https://doi.org/10.1016/j.synthmet.2017.11.006.

[43] L. Pilan, Tailoring the performance of electrochemical biosensors based on carbon nanomaterials via aryldiazonium electrografting, Bioelectrochem. 138 (2021) 107697. https://doi.org/10.1016/j.bioelechem.2020.107697.

[44] B.D. Assresahegn, T. Brousse, D. Belanger, Advances on the use of diazonium chemistry for functionalization of materials used in energy storage systems, Carbon 92 (2015) 362-381. https://doi.org/10.1016/j.carbon.2015.05.030.

[45] N. Delaporte, R.L. Belanger, G. Lajoie, M. Trudeau, K. Zaghib, Multi-carbonyl molecules immobilized on high surface area carbon by diazonium chemistry for energy storage applications, Electrochim. Acta 308 (2019) 99-114. https://doi.org/10.1016/j.electacta.2019.04.012.

[46] R. Khan, Y. Nishina, Covalent functionalization of carbon materials with redox-active organic molecules for energy storage, Nanoscale 13 (2021) 36-50. https://doi.org/10.1039/d0nr07500k.

[47] A. Vacca, M. Mascia, S. Rizzardini, S. Palmas, L. Mais, Coating of gold substrates with polyaniline through electrografting of aryl diazonium salts, Electrochim. Acta 126 (2014) 81-89. https://doi.org/10.1016/j.electacta.2013.08.187.

[48] J. Lyskawa, D. Belanger, Direct modification of a gold electrode with aminophenyl groups by electrochemical reduction of in situ generated aminophenyl monodiazonium cations, Chem. Mater. 18 (2006) 4755-4763. https://doi.org/10.1021/cm060752d.

[49] L.M. Santos, J. Ghilane, C. Fave, P.C. Lacaze, H. Randriamahazaka, L.M. Abrantes, J.C. Lacroix, Electrografting polyaniline on carbon through the electroreduction of diazonium salts

and the electrochemical polymerization of aniline, J. Phys. Chem. C 112 (2008) 16103-16109. https://doi.org/10.1021/jp8042818.

[50] L. Pilan, M. Raicopol, A. Pruna, V. Branzoi, Polyaniline/carbon nanotube composite films electrosynthesis through diazonium salts electroreduction and electrochemical polymerization, Surf. Interf. Anal. 44 (2012) 1198-1202. https://doi.org/10.1002/sia.4920.

[51] A. Jacques, M.M. Chehimi, C. Poleunis, A. Delcorte, J. Delhalle, Z. Mekhalif, Grafting of 4-pyrrolyphenyldiazonium in situ generated on NiTi, an adhesion promoter for pyrrole electropolymerisation?, Electrochim. Acta 211 (2016) 879-890. https://doi.org/10.1016/j.electacta.2016.06.060.

[52] V. Stockhausen, J. Ghilane, P. Martin, G. Trippe-Allard, H. Randriamahazaka, J.C. Lacroix, Grafting oligothiophenes on surfaces by diazonium electroreduction: A step toward ultrathin junction with well-defined metal/oligomer interface, J. Am. Chem. Soc. 131 (2009) 14920-14927. https://doi.org/10.1021/ja9047009.

[53] D. Chhin, D. Polcari, C. Bodart-Le Guen, G. Tomasello, F. Cicoira, S.B. Schougaard, Diazonium-Based Anchoring of PEDOT on Pt/Ir Electrodes via Diazonium Chemistry, J. Electrochem. Soc. 165 (2018) G3066. https://doi.org/10.1149/2.0061812jes.

[54] F. Bekkar, F. Bettahar, I. Moreno, R. Meghabar, M. Hamadouche, E. Hernaez, J.L. Vilas-Vilela, L. Ruiz-Rubio, Polycarbazole and Its Derivatives: Synthesis and Applications. A Review of the Last 10 Years, Polymers 12 (2020) 2227. https://doi.org/10.3390/polym12102227.

[55] V. Nayana, B. Kandasubramanian, Polycarbazole and its derivatives: progress, synthesis, and applications, J. Polym. Res. 27 (2020) 285. https://doi.org/10.1007/s10965-020-02254-7.

[56] S.H. Kim, S.I. Hong, Synthesis of aromatic polyamide from N-methylcarbazole-3,6-diamine and diacid chloride, Polymer Korea 9 (1985) 219-229. ISSN 2234-8077.

[57] A.J. Downard, M.J. Prince, Barrier properties of organic monolayers on glassy carbon electrodes, Langmuir 17 (2001) 5581-5586. https://doi.org/10.1021/la010499q.

[58] B. Lesiak, L. Kövér, J. Tóth, J. Zemek, P. Jiricek, A. Kromka, N. Rangam, C sp2/sp3 hybridisations in carbon nanomaterials – XPS and (X)AES study, Appl. Surf. Sci. 452 (2018) 223-231. https://doi.org/10.1016/j.apsusc.2018.04.269.

[59] S. Samanta, I. Bakas, A. Singh, D.K. Aswal, M.M. Chehimi, In Situ Diazonium-Modified Flexible ITO-Coated PEN Substrates for the Deposition of Adherent Silver–Polypyrrole Nanocomposite Films, Langmuir 30 (2014) 9397-9406. https://doi.org/10.1021/la501909r.

[60] J.M. Stillahn, K.J. Trevino, E.R. Fisher, Deposition of Amorphous CN_x Materials in BrCN Plasmas: Exploring Adhesion Behavior as an Indicator of Film Properties, ACS Appl. Mater. Interf. 3 (2011) 1402-1410. https://doi.org/10.1021/am101282y.

[61] M.P. Schwartz, R.J. Hamers, Reaction of acetonitrile with the silicon (001) surface: A combined XPS and FTIR study, Surf. Sci. 601 (2007) 945-953. https://doi.org/10.1016/j.susc.2006.11.035.

[62] N. Graf, E. Yegen, T. Gross, A. Lippitz, W. Weigel, S. Krakert, A. Terfort, W.E.S. Unger, XPS and NEXAFS studies of aliphatic and aromatic amine species on functionalized surfaces, Surf. Sci. 603 (2009) 2849-2860. https://doi.org/10.1016/j.susc.2009.07.029.

[63] Y.N. Liu, X. Zhou, X. Wang, K. Liang, Z.K. Yang, C.C. Shen, M. Imran, S. Sahar, A.W. Xu, Hydrogenation/oxidation induced efficient reversible color switching between methylene blue and leuco-methylene blue, RSC Adv. 7 (2017) 30080-30085. https://doi.org/10.1039/C7RA04498D.

[64] C. Luo, X. Ji, S. Hou, N. Eidson, X. Fan, Y. Liang, T. Deng, J. Jiang, C. Wang, Azo Compounds Derived from Electrochemical Reduction of Nitro Compounds for High Performance Li-Ion Batteries, Adv. Mater. 30 (2018) 1706498. https://doi.org/10.1002/adma.201706498.

[65] S. Carniato, F. Rochet, J.-J. Gallet, F. Bournel, G. Dufour, C. Mathieu, S. Rangan, DFT calculations of XPS/NEXAFS and IR spectra to elucidate the reaction products of acetonitrile with Si(001)-2×1, Surf. Sci. 601 (2007) 5515-5525. https://doi.org/10.1016/j.susc.2007.09.039.

[66] T. Menanteau, M. Dias, E. Levillain, A.J. Downard, T. Breton, Electrografting via Diazonium Chemistry: The Key Role of the Aryl Substituent in the Layer Growth Mechanism, J. Phys. Chem. C 120 (2016) 4423-4429. https://doi.org/10.1021/acs.jpcc.5b12565.

[67] S. Sadki, P. Schottland, N. Brodie, G. Sabouraud, The mechanisms of pyrrole electropolymerization, Chem. Soc. Rev. 29 (2000) 283-293. https://doi.org/10.1039/a807124a.

[68] E. Contal, S. Lakard, F. Dumur, B. Lakard, Investigation of polycarbazoles thin films prepared by electrochemical oxidation of 3- and 9-substituted carbazoles, Progr. Org. Coat. 162 (2022) 106563. https://doi.org/10.1016/j.porgcoat.2021.106563.

[69] V. Karabozhikova, V. Tsakova, C. Lete, M. Marin, S. Lupu, Poly (3, 4-ethylenedioxythiophene)-modified electrodes for tryptophan voltammetric sensing. J. Electroanal. Chem. 848 (2019) 113309. https://doi.org/10.1016/j.jelechem.2019.113309.

[70] F. Gao, J. Mu, Z. Bi, S. Wang, Z. Li, Recent advances of polyaniline composites in anticorrosive coatings: a review, Progr. Org. Coat. 151 (2021) 106071. https://doi.org/10.1016/j.porgcoat.2020.106071.

[71] M. Ates, A.S. Sarac, C.M. Turhan, N. Ayaz, Polycarbazole modified carbon fiber microelectrode: Surface characterization and dopamine sensor, Fibers Polym. 10 (2009) 46–52 (2009). https://doi.org/10.1007/s12221-009-0046-4.

[72] M. Lo, A.K.D. Diaw, D. Gningue-Sall, J.J. Aaron, M.A. Oturan, M.M. Chehimi, The role of diazonium interface chemistry in the design of high performance polypyrrole-coated flexible ITO sensing electrodes, Electrochemistry Communications 77 (2017) 14. https://doi.org/10.1016/j.elecom.2017.02.002.